Quantum Electronics **34**(7) 669 – 672 (2004)

FIBREOPTIC DEVICES

PACS numbers: 42.81.Pa; 42.55.Wd
DOI: 10.1070/QE2004v034n07ABEH002825

Enhancement of the sensitivity of a recirculation fibre ring interferometer with pulsed pumping of an intracavity optical erbium-doped fibre amplifier

E.I. Alekseev, E.N. Bazarov, V.P. Gubin, A.I. Sazonov, N.I. Starostin, A.I. Usov

Abstract**. The signal sensitivity and detection capability of a recirculation fibre ring interferometer (RFRI) are studied experimentally upon pulsed pumping of an intracavity ytterbium-sensitised erbium-doped fibre amplifier (YEDFA). It is shown that the number of effective circulations of light in the ring resonator can be substantially increased in the transient regime above the self-excitation threshold when, however, lasing has yet no time to develop. It is found that the required transient regime is achieved due to the self-restriction (drop) of amplification in YEDFA caused by the saturation of the active medium with increasing radiation power in the resonator. The increase in the signal sensitivity of the RFRI and its detection capability by factors of 25 and 4, respectively, is demonstrated in the pulsed regime of the YEDFA.**

Keywords*: recirculation interferometer, fibre amplifier, pulsed pumping.*

The high-Q ring resonator in recirculation fibre ring interferometers (RFRIs) is pumped by broadband radiation, which drastically reduces the effect of many factors on the accuracy of phase measurements [1]. The parameters of an RFRI are determined by the number of efficient recirculations of radiation trains in the ring resonator, whose perimeter L is much greater than the coherence length l_c of radiation. The number of recirculations can be considerably increased by compensating partially for resonator losses with the help of an intracavity optical amplifier [2 – 4]. In fact, due to the presence of an active element (amplifier) inside the ring resonator, such an RFRI is a regenerative system, i.e., the system in which lasing appears when losses are completely compensated, which violated the normal operation of the interferometer.

However, the best characteristics of the RFRI are achieved when amplification is as much as possible close to the lasing threshold. Such a regime can be obtained, in particular, by stabilising the optical gain near the lasing threshold in the continuous operation regime of the amplifier. Another approach is the use of the pulsed regime of the amplifier. In this case, the amplifier with the enhanced gain is switched for a certain time during which light performs many round trips in the ring resonator, but lasing has yet no time to develop [5, 6], and then the amplifier is switched off. The pulsed modulation of the gain can be performed by different methods, for example, by modulating the pump power of the optical amplifier or modulating losses in the ring resonator.

The aim of this paper is the experimental study of the possibility of increasing the RFRI sensitivity by using the pulsed modulation of the pump power of an intracavity ytterbium – erbium-doped fibre amplifier (YEDFA).

Experiments were performed using the setup shown in Fig. 1, which represents the RFRI prototype with a superfluorescent fibre source (SFS) and an intracavity YEDFA [4]. As the YEDFA, we used a commercial $\mathrm{Yb}^{3+}:\mathrm{Er}^{3+}$-doped silica fibre amplifier with an aluminosilcate core manufactured at the IRE Polyus Scientific and Technical Association. Ytterbium ions at a high concentration, which strongly absorb pump radiation, serve to enhance (sensitise) the pump efficiency of erbium ions [6]. Pumping was performed at 0.98 μm by a multimode laser diode whose radiation was symmetrically coupled into both ends of the active fibre. Because the $^2F_{5/2}$ and $^2F_{7/2}$ energy levels of ytterbium are very close to the $^4I_{11/2}$ and $^4I_{15/2}$ working levels of erbium (Fig. 2), the efficient energy transfer from ytterbium to erbium occurs, providing the required amplifi-

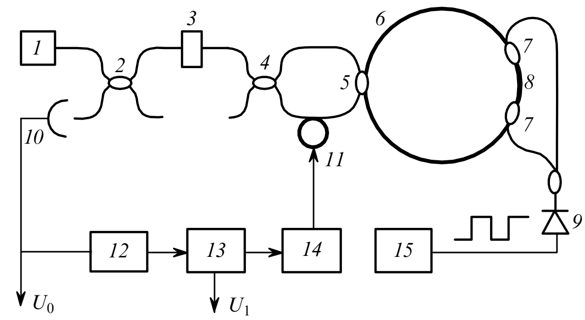

Figure 1. Scheme of the experimental setup: (*1*) SFS; (*2*, *4*, *5*) directional couplers; (*3*) polariser; (*6*) ring resonator; (*7*) multiplexer couplers; (*8*) active fibre; (*9*) laser diode; (*10*) photodiode; (*11*) phase modulator; (*12*) band-pass filter; (*13*) synchronous detector; (*14*) sine wave generator; (*15*) pulse generator.

E.I. Alekseev, E.N. Bazarov, V.P. Gubin, A.I. Sazonov, N.I. Starostin, A.I. Usov Institute of Radio Engineering and Electronics, Fryazino Division, Russian Academy of Sciences, pl. Akad. Vvedenskogo 1, 141120 Fryazino, Moscow region, Russia; e-mail: nis229@ire216.msk.su; http:\\fire.relarn.ru

Received 19 February 2004; revision received 27 April 2004
Kvantovaya Elektronika **34** (7) 669 – 672 (2004)
Translated by M.N. Sapozhnikov

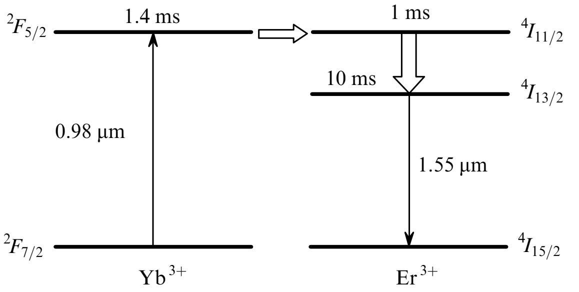

Figure 2. Energy level diagram of ytterbium and erbium.

cation at 1.55 μm at a comparatively low pump power. The typical gain of the YEDFA was 5 dB. It is shown below that this pump scheme determines the properties of the pulsed regime of the RFRI. Pulsed operation was performed at the pulse repetition rate F_p and duration τ_p of current pulses from the pump diode, whose values were chosen in preliminary experiments.

The ring resonator of the RFRI was made of a Panda single-mode ($\lambda \simeq 1.55$ μm) anisotropic fibre of length $L = 200$ m in the form of a coil of diameter $D = 125$ mm.

A signal was detected by a synchronous detector with a band-pass filter at the input. The output signal of the RFRI was detected at the frequency $f_m = 291$ kHz of the first harmonic of an auxiliary harmonic phase modulation of radiation. The band-pass filter tuned to this frequency provided the 60-dB suppression of harmonics of the pulsed modulation of radiation, which could interfere with the useful signal. The low-pass filter at the synchronous detector output had the bandpass $\Delta F = 1$ Hz. The transfer coefficient of the synchronous detector for the pulsed input signal depended on the off–duty ratio of detected radio pulses and was determined experimentally.

Oscillograms of the voltage U_0 at the output of the RFRI detector for different durations τ_p of the pump current pulses of the YEDFA are presented in Figs 3 and 4 (stable regimes) and Fig. 5 (unstable regime). The output voltage in the stable regime represents bell-shaped video pulses with the amplitude $U \approx 10$ V and the FWHM $\tau \approx 60$ μs on which the modulation components of the harmonics f_m are superimposed (radio pulses in Figs 3 and 4 poorly visible). To determine the signal sensitivity, the RFRI was used as a sensor of the angular velocity.

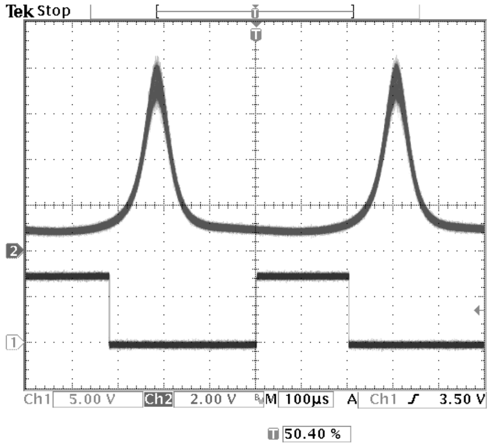

Figure 3. Output signal of the photodetector for $F_p = 2000$ Hz, and $\tau_p = 200$ μs.

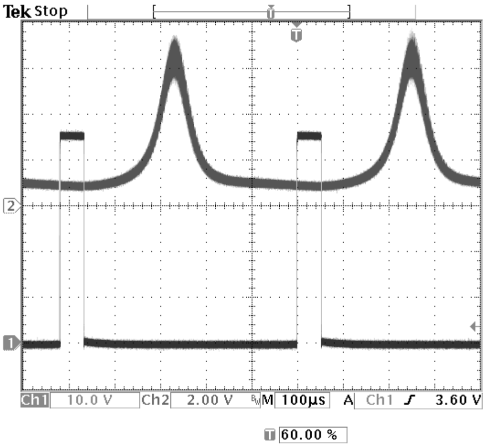

Figure 4. Output signal of the photodetector for $F_p = 2000$ Hz, and $\tau_p = 50$ μs.

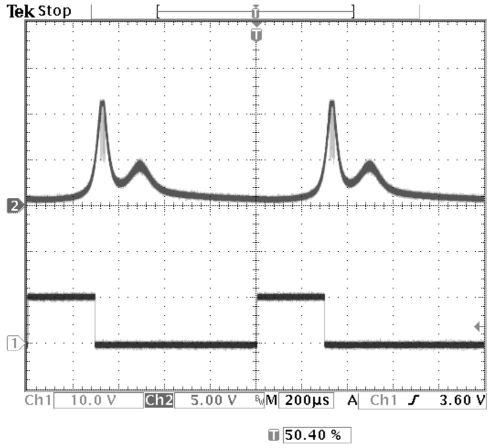

Figure 5. Output signal of the photodetector for $F_p = 1000$ Hz and $\tau_p = 300$ μs.

In the absence of the rotation of the RFRI resonator around the axis perpendicular to the plane of coils, only even harmonics f_m are present. In the case of rotation, odd harmonics appear whose amplitudes are proportional to Ω at small angular velocities Ω. In this experiment, the useful signal is the first harmonic whose amplitude is small (for $\Omega = 130$ deg h^{-1}) and is not seen in figures. The data presented in Figs 3 and 4 were obtained for maximum admissible pump currents at which a stable operation of the RFRI is observed. When the pump current was further increased, the RFRI operation becomes unstable and the second and next pulses appear (Fig. 5). The characteristic features of these regimes are a weak dependence of the shape and duration of the video pulse of the useful signal on the repetition rate and off–duty ratio of pump pulses, the almost identical shape of the leading and trailing edges of the video pulse in the absence of a noticeable flat top, as well as video pulse delay with respect to the pump pulse.

The oscillograms presented above can be interpreted as follows (Fig. 6). After the switching on of the pump pulse (Fig. 6a), the population inversion of the working levels of erbium begins to increase (the $^4I_{13/2} - ^4I_{15/2}$ transition,

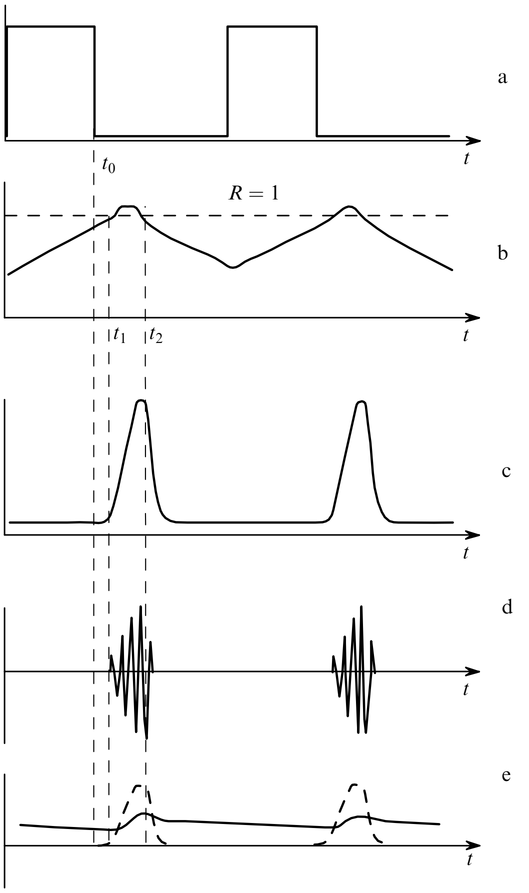

Figure 6. Illustration of the RFRI operation with pulsed pumping of the EDFA: the EDFA pump current (a), transfer coefficient in the ring resonator (b), radiation power in the resonator (c), input signal of the phase detector (d), and output signal of the phase detector (e).

Fig. 2), resulting in the increase in the YEDFA gain g. The signal sensitivity of the RFRI is determined by the number of effective circulations of radiation in the ring resonator, which in turn depends on the amplitude transfer coefficient $R = ag$ per a round trip in the resonator [2]. Here, $a \approx 0.6$ is the transfer coefficient in the ring determined by passive losses, including output coupling losses. Therefore, R increases with increasing g (Fig. 6b), this increase being continued after the end of the pump pulse at the moment t_0 due to the transfer of energy accumulated at the $^2F_{5/2}$ level of the Yb^{3+} ions. For $R > 1$, which takes place at the moment t_1, the field intensity in the resonator rapidly increases (Fig. 6c). This leads to the saturation of the working transition in erbium, As a result, the gain begins to decrease and it becomes lower than the lasing threshold at the moment t_2 (in this case, $R < 1$). Beginning from this moment, the field intensity in the resonator rapidly decreases (Fig. 6c). The stationary lasing has no time to develop during the video pulse duration because the drop of the gain (population inversion) occurs, after which the pump energy accumulated in ytterbium ions is not sufficient to provide a new growth of the field. However, many circulations of radiation in the resonator are provided during the video pulse.

Note that these processes occur in the regime of 'automatic' control (the parameters of a system with a feedback are determined by the lifetimes of the energy levels of the medium and the Q factor of the optical resonator), which provides a weak dependence of the video pulse shape (more exactly, of its width at the base) on the pump–pulse parameters (Figs 3 and 4). Of course, in the case of intense pumping, it can occur that the accumulated energy in ytterbium ions remaining after the gain drop will be sufficient for the generation of the second (and even third) field pulses in the resonator (Fig. 5).

As mentioned above, the output signal of the RFRI consists of video pulses of a certain power propagating with the pulse repetition rate F_p (Fig. 6c) and of radio pulses superimposed on the video pulses and dependent on the angular velocity, which have the shape shown in Fig. 6d after propagation through the band-pass filter. Note that the envelope of these pulses does not coincide with that of video pulses. Radio pulses arrive at the synchronous detector, which, for $F_p \gg \Delta F$, produces the dc voltage $U_1(\Omega)$ proportional to the average value of the radio-pulse envelope. The transfer coefficient of the synchronous detector was measured to be $K = 43$ for $f_m = 291$ kHz, $F_p = 2000$ Hz, and $\tau_p = 200$ μs. In the regime of detecting a continuous radio signal at the frequency 291 kHz, te transfer coefficient was $K = 94$.

By using the experimental data, we compare the signal sensitivities and detection capabilities of the RFRI in the continuous and pulsed regimes. The signal sensitivity of the RFRI (its response to small rotations) Q_s is proportional to the $U_1(\Omega)/\Omega$ ratio. Note that it was measured in both regimes for the same parameters of the electronic signal processing unit. The detection capability (threshold sensitivity) of the RFRI was estimated from the expression $\Omega_{\min} = U_{1n}/Q_s$, where U_{1n} is the root-mean-square noise voltage at the synchronous detector output in the absence of phase modulation, which is determined by the output noise of the RFRI in the absence of rotation. The value of U_{1n} was measured in both regimes for the same parameters of the electronic unit as well. Comparison was performed in the near-threshold operating regime of the RFRI. The values of Q_s were 5.3 and 62 mV deg^{-1} h for the continuous and pulsed regimes, respectively. After reduction to the same value of the transfer coefficient of the synchronous detector, these values were 5.5 and 135 mV deg^{-1} h, respectively. In these regimes, $\Omega_{\min}$ was 0.15 and 0.034 deg h$^{-1/2}$ Hz$^{-1/2}$, respectively. Therefore, Q_s increased by a factor of 25, while $Q_{\min}$ decreased by a factor of 4.4. Note also that the maximum voltage across the photodetector (U_0 in the pulsed regime and U_p in the pulsed regime) increased in the pulsed regime approximately by a factor of 12.

We also measured the dependences of the signal sensitivity on the YEDFA gain in the continuous and pulsed regimes of the RFRI. They are presented in Fig. 7, where on the abscissa the maximum voltages across the photodetector are plotted in the continuous and pulsed regimes. A comparatively weaker dependence for the pulsed regime can be explained as follows. We can assume that the RFRI sensitivity is proportional to the product of the pulse amplitude by the number of effective circulations during the pulse. It seems that the number of effective circulations increases with decreasing U_p, which is demonstrated by a flatter top of the pulse with lower amplitude [it follows from a comparison of the shapes of the first (large) and second pulses in Fig. 5]. As a result, as the YEDFA gain decreases, the reduction of the sensitivity due to a decrease in U_p is partially compensated by the increase in the number of

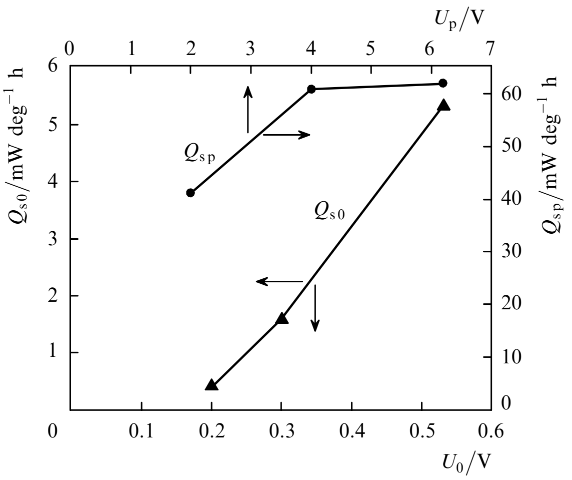

Figure 7. Dependences of the signal sensitivity for the continuous (Q_{s0}) and pulsed (Q_{sp}) amplification regimes of the YEDFA (voltages across the photodetector).

effective circulations. Note that video pulses retain their symmetric shape at any values of U_p.

Therefore, the pulsed regime considered here allows one to increase substantially the signal sensitivity of the RFRI. This regime also provides, in principle, an increase in the RFRI detection capability determined by the radiation noise and measured in the absence of phase modulation of radiation. Note, however, that under the working conditions (when phase modulation is switched on), the enhanced noise level is observed, which is probably caused by random variations in the initial phases of radio pulses during their formation at each pump pulse. The mechanism of this noise and the method of its suppression require further studies.

The results obtained above show that the number of effective circulations of radiation in the ring resonator noticeably increases in the pulsed regime. The number of effective circulations can be roughly estimated as $m \approx \tau/\tau_1 = 60$, where $\tau \approx 60$ μs is the FWHM of stable pulses and $\tau_1 = nL/c \approx 1$ μs is the time of one circulation. Assuming that $m \approx F$, where $F = \pi R/(1 - R^2)$ is the finesse of the optical resonator, we estimated the maximum transfer coefficient as $R_{\max} = 0.975$ in the continuous regime, whose sensitivity is equivalent to that of the pulsed regime for the given experimental setup. Of course, the real pulsed regime cannot be described by a fixed value of R because R changes in time and typically exceeds unity. Note that in a real pre-threshold regime $R = 0.9$ for the given setup.

Therefore, we have studied experimentally the signal sensitivity and detection capability of the RFRI upon pulsed pumping of an intracavity ytterbium-synthesised EDFA. We have shown that the number of effective circulations of light in the ring resonator can be substantially increased in the transient regime above the self-excitation threshold when, however, lasing has yet no time to develop. We have found that the required transient regime is achieved due to the self-restriction (drop) of the YEDFA gain because of the saturation of the active medium with increasing field in the resonator. We have demonstrated the increase in the signal sensitivity and detection capability of the RFRI by factors of 25 and 4, respectively, in the pulsed regime of the YEDFA.

Acknowledgements. The authors thank V.P. Gapontsev and I.E. Samartsev for their support of this study. This work was partially supported by the Ministry of Science (Grant No. 01.40.01.08.02).

References

1. Farhadiroushan M., Giles I.P., Youngquist R.C. *Proc. SPIE Int. Soc. Opt. Eng.*, **719**, 178 (1986).
2. Yu A., Siddiqui A.S. *Electron. Lett.*, **28**, 1778 (1992).
3. Kringlebotn J.T., Blotekjaer K. *J. Lightwave Technol.*, **12**, 573 (1994).
4. Alekseev E.I., Bazarov E.N., et al. *Kvantovaya Elektron.*, **31**, 1113 (2001) [*Quantum Electron.*, **31**, 1113 (2001)].
5. Chen D.N., Motoshima K., Downs M.M., Desurvire E. *IEEE Photon. Technol. Lett.*, **4**, 813 (1992).
6. Desurvire E. *Erbium-Doped Fiber Amplifiers: Principles and Applications* (New York: A Wiley-Interscience Publication, 1994).